Drift effects in SOLPS-ITER simulations for the TCV divertor upgrade

M. Wensing[1], H. De Oliveira[1], C. Dodson[1], B. P. Duval[1], O. Février[1], A. Fil[2], D. Galassi[1], J. Loizu[1], L. Martinelli[1], R. Maurizio[1], H. Reimerdes[1], C. Theiler[1], A. Thornton[2], K. Verhaegh[1,3], M. Wischmeier[4], the EUROfusion MST1[5] team and the TCV team[6]

[1] *EPFL - Swiss Plasma Center (SPC), Lausanne, Switzerland,* [2] *CCFE, Culham Science Centre, Abingdon, Oxon, OX14 3DB, UK,* [3] *University of York - Plasma Institute, York, United Kingdom,* [4] *Max-Planck-Institut für Plasmaphysik, Garching, Germany,* [5] *See author list of B. Labit et al 2019 Nucl. Fusion 59 086020,* [6] *See author list of S. Coda et al 2019 Nucl. Fusion accepted (https://doi.org/10.1088/1741-4326/ab25cb)*

This contribution reports on the progress towards including drift effects in SOLPS-ITER simulations to assess power distribution and detachment onset in the light of the 2019 TCV divertor upgrade [1]. The installation of in-vessel gas baffles (Figure 1a) is predicted to increase the divertor neutral density by a factor ~ 5 and therefore facilitates the access to detachment [2]. The conditions for the onset of detachment at each strike point depend on the power entering each divertor leg and thus simulations must correctly include the power distribution between the inner and outer divertor that is greatly affected by scrape-off layer drifts. Surprisingly, the sharing of particles and heat between the targets in reversed field conditions is found to be shifted towards the outer target. This counter-intuitive flow pattern is due to an electric potential well below the X-point that occurs in high density reversed field simulations.

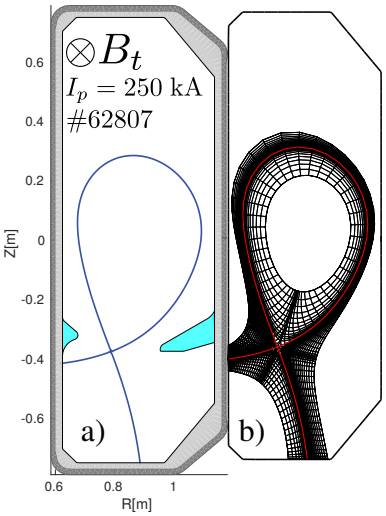

Figure 1: *a) Reference discharge with baffles, b) corresponding simulation grid.*

Comparison of reference simulations with experimental data

These SOLPS-ITER [3][4] simulations are performed for Ohmically heated, L-mode, density ramp discharges compatible with the baffle elements being installed on TCV (Figure 1a). Simulation parameters and reactions are summarised in [2]. The simulation grid is based upon an experimental equilibrium reconstruction (Figure 1b) extended radially towards the planned inner baffle tip. Neutrals are treated kinetically using Eirene. Initially, existing experimental data is compared with reference simulations excluding drift effects with special attention directed to qualitative differences from the simulation. Power is transferred through the core boundary to match the experimental power entering the scrape-off layer $P_{SOL} \approx 300$ kW. The simulated gas puff scan $\Gamma^{D_2}_{puff} = 4 - 10 \cdot 10^{20}$ D^0/s is compared for distinct times during the discharge based on the respective upstream densities (Figure 2a). Simulated upstream profiles, obtained with spatially constant and species-independent transport parameters ($D_\perp = 0.2$ m^2/s, $\chi_{i/e,\perp} = 1.0$ m^2/s), are in reasonable agreement with the measured Thomson scattering (TS) profiles. They yield a scrape-off layer width of $\lambda_{n_e} \approx 1.0$ cm, $\lambda_{T_e} \approx 0.8$ cm, slightly larger than experimentally observed. Interestingly, in the simulation T_e^u decreases as $\propto 1/n_e^u$, which is seen experimentally, albeit to a lesser extent. The simulation introduces carbon by sputter-

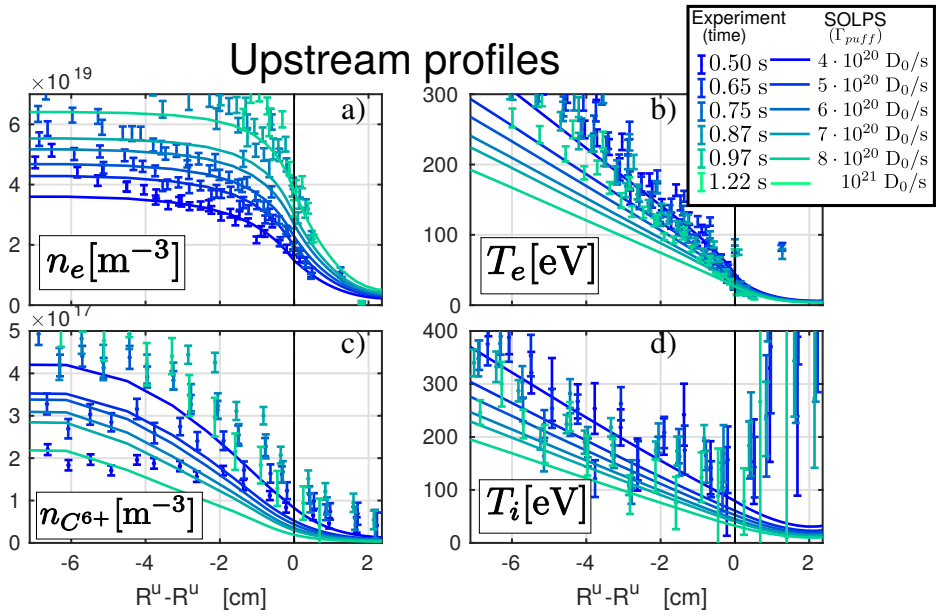

Figure 2: *Upstream profiles as diagnosed by TS and CXRS a) electron density, b) electron temperature, c) C^{6+}-density and d) ion temperature.*

ing from the plasma-facing components. The resulting upstream C^{6+}-density decreases with the upstream electron density, possibly related to the decrease of the core electron temperature which consequentially reduces ionisation. Charge-exchange spectroscopy (CXRS) shows an opposite trend (Figure 2c). The experimental increase of carbon density may be related to increased main chamber plasma-wall interaction as suggested in [5]. Comparison to target heat flux profiles, bolometer chord brightness, Balmer line brightness and the overall power balance shows generally qualitative agreement (not shown here).

Numerical instabilities encountered in drift cases

Including drift effects in many transport codes including SOLPS-ITER remains numerically challenging. Frequently encountered numerical instabilities are linked to the explicit solver. Drift simulations often impose a stricter upper limit on the simulation time step than simulations without drifts to prevent instabilities such as oscillations of the core's electric potential [6] often resulting in unacceptable computation time. Herein, we present another type of instability occurring in drift cases that causes an even stricter time step limit than core oscillations.

SOLPS-ITER computes a self-consistent description of the electric potential ϕ by solving the current continuity equation $\nabla \cdot \mathbf{j} = 0$. The electric current $\mathbf{j}$ includes contributions from diamagnetic drift, ion-neutral friction, viscosity, inertia, the parallel momentum balance and a so called anomalous current $j_\perp = \sigma_{AN} E_\perp$, i.e. an artificial term needed for convergence.

For TCV cases with drifts the emergence of periodic, stable oscillations in the electron density and the electric potential are observed at either of the targets, but most typically the outer one. These are phase shifted by $\pi/2$ and localised radially in the vicinity of the separatrix ($\sim$ 10 radial cells) extending about a centimetre in the direction towards the X-point ($\sim$ 3 poloidal cells). Several conditions are found to help suppress these oscillations: 1) strongly detached cases naturally show relatively flat target profiles for which radial electric fields are small, 2) small time steps dt, 3) high anomalous conductivity σ_{AN}, 4) increased distance between adjacent

radial cells at the separatrix (here: $dr^{ot}_{min} = 0.9$ mm$\rightarrow$ 1.4 mm). Simulations with 100 iterations starting from a non-oscillating state demonstrate that oscillations may rapidly emerge depending of the values of σ_{AN} and dt (Figure 3a,b).

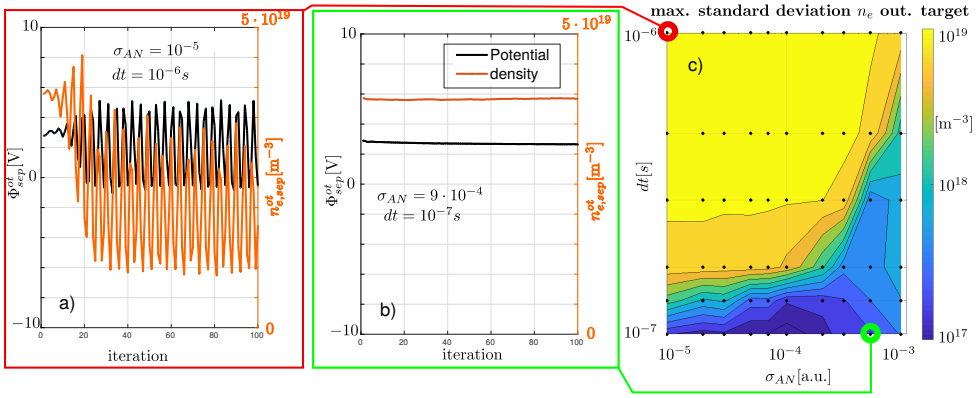

Figure 3: a) Oscillatory case (high dt, low σ_{AN}), b) stable case (low dt, high σ_{AN}), c) scan of σ_{AN}, dt demonstrates occurrence of outer target profile oscillations.

From these observations, a possible explanation for these oscillations is proposed. An initial perturbation of electric potential leads to $E \times B$ drift velocities of the order of the sound speed that causes a redistribution of the electron density at the target. Consequentially, the pressure is redistributed leading to a change in the electric potential.

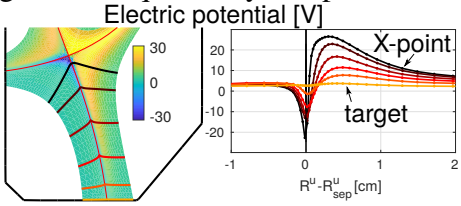

Figure 4: a) Electric potential ϕ in the divertor and b) its radial profiles.

Electric potential well in reversed field simulations

Converged reversed-field drift simulations show an unexpected electric potential minimum in the private flux region (PFR) below the X-point (Figure 4a,b) that can be attributed to the ion ∇B drift causing current flow into the core and high field side common flux region from the PFR region around the X-point. The charge balance along a PFR flux tube is maintained by parallel currents towards the X-point, analogous to the Pfirsch-Schlüter current on closed flux surfaces. Consequently, it is required that $\Phi_{X-point} < \Phi_{target}$. The well causes strong radial electric fields around the separatrix that distort the typical divertor $E \times B$ pattern near the separatrix (Figure 5a,b). The potential well is found to deepen with increasing upstream density, as the current connected with the ∇B drift $\mathbf{j}_{\nabla B} = en_e(\mathbf{v}^{\nabla B}_{ion} - \mathbf{v}^{\nabla B}_{e})$ is proportional to n_e.

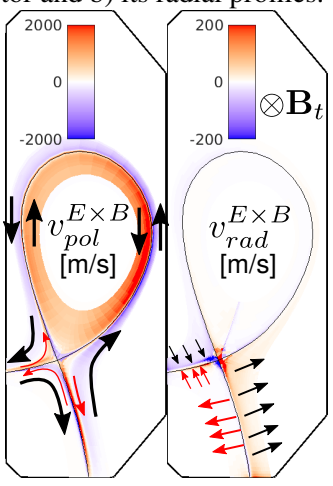

Figure 5: a) Poloidal and b) radial ExB flow pattern with $\rightarrow$-symbols indicating additional flows due to the presence of a PFR potential well.

Effect of drifts on in/out asymmetries

It is expected that increasing upstream density will lead to larger temperature gradients along field lines as the collisionality increases. This is generally thought to be concurrent with (often quadratic) increases

in the ion target current during the attached phase. A deviation from this trend, i.e. flattening and eventual roll-over of target current, is taken to be an indicator of detachment.

Typically, TCV core density ramps only show a clear roll-over at the outer target whereas the simulations give a simultaneous saturation of both target currents (Figure 6a). This is thought to be linked to an asymmetry of power entering the two divertors. However it is found, that accounting for drift effects in the reversed field case increases, contrary to the expectation, the heat and particle load at the outer target. This is a consequence of the modified near-SOL $E \times B$ flow pattern (Figure 6b,c) that convects heat and particles away from the inner strike point.

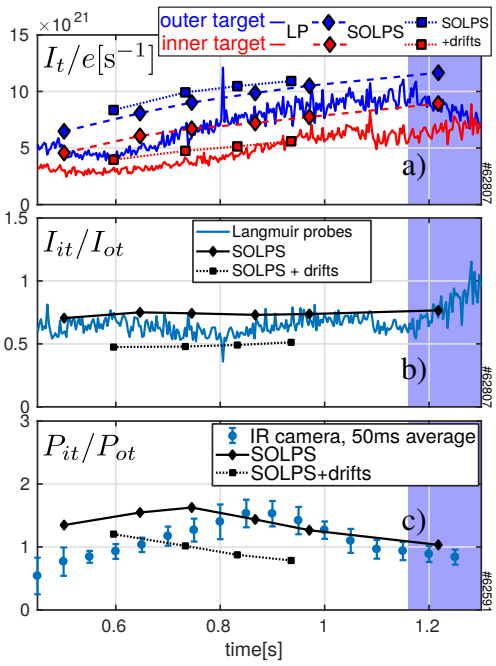

Figure 6: a) Target currents, b) inner/outer target current ratio and c) inner/outer target heat load ratio.

Conclusions and outlook

The comparison between SOLPS-ITER simulations and several diagnostics shows an overall satisfactory agreement with a few notable exceptions. The main short-comings of the simulations are 1) an insufficient target current roll-over at the outer target and 2) an opposite trend in core carbon density accumulation with increasing density. The lack of target current roll-over suggests that physical processes are missing in the simulation (molecular effects?, upstream pressure decrease?). Countermeasures to overcome target oscillations linked with drift cases were addressed. Surprisingly, the sharing of heat load between the targets in reversed field conditions is found to be shifted towards the outer target. This counter-intuitive flow pattern is explained by the formation of an electric potential well below the X-point at high densities. It results from the ∇B current towards the core and the consequential parallel divertor currents. Future work will be dedicated to further analysis of the potential well and the comparison of baffled and unbaffled cases in forward and reversed field.

References

[1] A. Fasoli, and the TCV team, *TCV Heating and Divertor Upgrades*, Fusion Energy Conference 2018
[2] M. Wensing et al, Plasma Phys. Control. Fusion, https://doi.org/10.1088/1361-6587/ab2b1f, 2019
[3] S. Wiesen et al., J. Nucl. Mat. 463, 480-484, 2015
[4] X. Bonnin et al., Plasma Fusion Res. 11, 1403103
[5] M. Wischmeier et al., *Enhanced main chamber wall interaction as an explanation for anomalous divertor detachment on TCV*, 32nd EPS Conference, Tarragona, 2005
[6] E. Kaveeva et al., Nucl. Fusion 58, 126018, 2018

This work has been carried out within the framework of the EUROfusion Consortium and has received funding from the Euratom research and training programme 2014 - 2018 and 2019 - 2020 under grant agreement No 633053. The views and opinions expressed herein do not necessarily reflect those of the European Commission.